Phosphate Oxygen Isotope Fingerprints of Past Biological Activity in the Atacama Desert

Ye Wang[a1*], *Ghazal Moradi*[bc1], *Erwin Klumpp*[b], *Christian von Sperber*[d], *Federica Tamburini*[e], *Benedikt Ritter*[f], *Barbara Fuentes*[g], *Wulf Amelung*[ab], *Roland Bol*[b]

[a] Institute of Crop Science and Resource Conservation - Soil Science and Soil Ecology, University of Bonn, 53115 Bonn, Germany

[b] Agrosphere (IBG-3), Institute of Bio- and Geosciences, Forschungszentrum Jülich GmbH, Germany

[c] Institute for Environmental Research, Biology 5, RWTH Aachen University, Worringerweg 1, 52074 Aachen, Germany

[d] Department of Geography, McGill University, Montreal QC H3A 0B9, Canada

[e] Institute of Agricultural Science, ETH Zurich, 8315 Lindau, Switzerland

[f] Institute of Geology and Mineralogy, University of Cologne, 50675 Cologne, Germany

[g] Laboratorio de Tecnología de Membranas, Medio Ambiente y Biotecnología, Departamento de Ingeniería Química, Universidad Católica del Norte, Antofagasta, Chile

*** Corresponding author: Ye Wang, yewang@uni-bonn.de, Tel: +49 (0)228732981**

[1] These authors contributed equally

ABSTRACT

The Atacama Desert (Chile) is one of driest places on Earth, with a hyper-arid climate and less than 2mm yr^{-1} precipitation; nevertheless, it has experienced rare periods of sporadic rainfall. These periods shortly enhanced vegetation growth and microbial activity, which must have utilized major nutrients such as phosphorus (P). However, any biological cycling of P involves an oxygen exchange with water, which should now reside in the hyperarid soils as tracer of life. In order to identify such evidences, we performed sequential P fractionation and analyzed the oxygen isotope composition of HCl-extractable phosphate ($\delta^{18}O_{HCl\text{-}P}$) in the surface soil (0-15 cm) of a climatic gradient along the rising alluvial fans of the Central Depression to the Precordillera, Chile. At the driest sites, the $\delta^{18}O_{HCl\text{-}P}$ values were constant with depth and deviated from biologically-driven isotopic equilibrium. In contrast, we observed a considerable increase of $\delta^{18}O_{HCl\text{-}P}$ values below the soil surface at less arid sites, where some isotope values were even within the range of full isotopic equilibrium with biologically cycled phosphate. For the latter sites, this points to most efficient biological P cycling right below the uppermost surface of the desert. Critically, the absolute concentrations of this biologically cycled P exceeded those of P potentially stored in living microbial cells by at least two orders of magnitude. Therefore, our data provides evidence that $\delta^{18}O_{HCl\text{-}P}$ values trace not recent but past biological activity, making it a powerful tool for assessing the existence, pathways and evolution of life in such arid ecosystems on earth and, thus, potentially on other planets such as Mars.

1. INTRODUCTION

The Atacama Desert has been known as a long-term arid to hyper-arid desert that experienced rare periods of rainfall that temporarily enhanced vegetation growth and soil microbial activity (Schulze-Makuch et al., 2018). Its extension is bound and restricted by the Andes to the east and the Pacific Ocean to the west (Fig. 1), and it stretches for more than 3000 km from southern Peru in the north to south of Copiapo (Pinto et al., 2006). Predominant arid conditions exist along the coast, above the coastal cliff (Coastal Cordillera), and on the lower-elevated levels of the western Andean foreslope (Central Depression, parts of the Precordillera). Aridity increases towards the hyper-arid core (areas with less than 2mm yr^{-1} and preservation of Miocene surfaces. see Ritter et al. 2018), which is at present restricted to an area covering parts of the Coastal Cordillera and Central Depression, between 19-23°S. Precipitation increases by 1-2 orders of magnitude towards the east where the Andes increase in height (Fig.1, Houston, 2006). Three major forcing factors are responsible for the desertification and aridification: (1) the position of the Atacama Desert at the subtropical high-pressure belt, in a zone of descending stable air, which could have been established since the late Jurassic (Hartley et al., 2005); (2) the subduction of the Nazca Plate under the South American Plate, which led to the uplift and evolution of the Central Andes, implementing a significant rain-shadow effect for Atlantic air masses (Houston and Hartley, 2003); and (3) the establishment of the cold Humboldt Current to the west of the Atacama Desert, inhibiting moisture uptake of onshore winds (Hartley and Chong, 2002). To date, there is a wide range of proposed ages for the onset of hyperaridity in the Atacama Desert from the Pliocene to the Miocene (Hartley and Chong, 2002; Rech et al., 2003; Dunai et al., 2005; Nishiizumi et al., 2005; Latorre et al., 2006; Rech et al., 2006; Nester et al., 2007; Evenstar et al., 2009; Jordan et al., 2014; Ritter et al. 2018; Dunai et al., 2020).

The alluvial fans of the northern Atacama are similar to presumably water-driven morphological features on Mars (Morgan et al., 2014). Intense deposition and erosion cycles created these fans. Terrestrial cosmogenic nuclide exposure ages from these alluvial fans (north of Quebrada Aroma) indicate several phases of surface activity and subsequent inactivity (Quade et al., 2008). At present, surface drainage bypass by the Quebrada Aroma spanning from the arid Precordillera of the Andes towards the hyper arid core of the desert, preserved upslope surfaces of the Aroma transect, which are devoid of any signs of recent surface drainage. Moreover, a well-developed desert pavement on a calcium-sulphate rich soil, promoted by atmospheric deposition, protects the underlying layers (Anderson et al., 2002; Ewing et al., 2006; Evenstar et al. 2009). The layers beneath the uppermost soil surface might hold evidence of life buried by aeolian dust, which might also be the case on Mars (Navarro-González et al., 2003).

A widely used method to detect and measure the distribution of geochemical versus biologically-related P pools in soils is the sequential P fractionation (Hedley et al., 1982). This method relies on the concept that only readily extractable P is biologically available, while harsher extraction steps release P that is less available to organisms. Phosphates immobilize in soil with increasing time by occlusion within oxides and aggregates and precipitation with Ca minerals (Gérard, 2016). Thus, past traces of life may not necessarily be found in readily available P pools, but preserved in P fractions that are only prone to extraction by harsher reagents, e.g., by HCl (Helfenstein et al., 2018). The oxygen isotopic composition of phosphate ($\delta^{18}O_P$) provides a proxy for distinguishing between geochemically and biologically cycled P forms and thus determining the importance of biological processes in soils (Blake et al., 2001; Tamburini et al., 2012). The combination of these two approaches has provided insights into P cycling in soils in a variety of environmental settings (Tamburini et al., 2012; Amelung et al., 2015; Bauke et al., 2017).

The applicability of the $\delta^{18}O_P$ method stems from the stability of P-O bond in phosphate under abiotic conditions at average temperatures at the Earth surface (Liang and Blake, 2007; Jaisi et al., 2010). Indeed, only biological processes driven by enzymes can break the P-O bond and cause oxygen exchange between phosphate and ambient water either with equilibrium or kinetic isotope fractionation effects (Blake et al., 2001). Microorganisms take up inorganic P, which participates in several metabolic processes inside the cells. Intracellular pyrophosphatase enzymes catalyze the hydrolysis of pyrophosphate (P_2O_7, an important by-product of several metabolic processes) into two inorganic phosphate molecules, leading to a temperature-dependent equilibrium fractionation between oxygen in phosphate and ambient water (Blake et al., 2005; von Sperber et al., 2017). Outside the cell, plants and microorganisms produce extracellular phosphatase enzymes that hydrolyze phosphoesters and release available P, leading to a kinetic fractionation of oxygen isotopes. Phosphatases incorporate one or more oxygen atoms into the newly formed inorganic phosphate, while the remaining oxygen atoms are inherited from the original organic P moiety (Liang and Blake, 2006; 2009; von Sperber et al., 2014; 2015).

Calcium carbonate minerals are the principal geochemical pool of P (operationally defined by the 1M HCl extract in the sequential P fractionation procedure) in alkaline soils (e. g. Aridisols; see Shen et al., 2020) and are considered to be a pool of unavailable P to plants and microorganisms. Although 1M HCl-extractable P is not directly engaged in biological cycling of P, its $\delta^{18}O_p$ composition might preserve the signal of soil P that was biologically cycled in the past (Amelung et al., 2015; Joshi et al., 2016). These secondary calcium minerals can form in the soil, co-precipitating P, that was previously biologically cycled, from the soil solution. It has been shown that the turnover time of HCl-P is from years to millennia, especially in arid environments with alkaline soils (Helfenstein et al., 2018). Thus, in certain environments, $\delta^{18}O_{HCl\text{-}P}$ might retain

a signal of biological P cycling, unlike other more bioavailable P pools with a short turnover time. Shen et al. (2020) sampled soils (soil depth, 10-20 cm) from five Atacama study sites along a latitudinal gradient from 22 to 28 °S and revealed that arid sites exhibit higher $\delta^{18}O_{PO4}$ values of soil Ca-P (19.5-25.3‰) and greater microbial P stocks compared to hyperarid sites. These data already demonstrated the utility of $\delta^{18}O_{PO4}$ values as indicative of biogeochemical cycling in an extremely dry environment. However, there is still a lack of information about estimation of the $\delta^{18}O_{HCl\text{-}P}$ biologically-driven isotopic equilibrium range for these dry environments and how the $\delta^{18}O_{HCl\text{-}P}$ value changes at different soil depths from surface to the subsurface along elevation transects of the Atacama Desert.

Here, we use the oxygen isotopes in phosphate combined with sequential P fractionation to study the history of phosphate in the hyper-arid environment of the Atacama Desert, where free water availability is the ultimate limiting factor for life (Navarro-González et al., 2003; Warren-Rhodes et al., 2006). Our research aim was to examine whether the $\delta^{18}O_{HCl\text{-}P}$ is outside of the calculated isotopic equilibrium range (which is expected if P derives only from weathered igneous parent material) or at equilibrium, as a result of biological activity. This methodology, if informative in the hyper-arid system of the Atacama Desert, might also offer options for tracing extraterrestrial life in meteorites or on Mars (Blake et al., 2001).

2. MATERIALS AND METHODS

2.1. Study area

The study area (the Aroma transect) is located on an alluvial fan in the north of Quebrada Aroma in northern Chile. The Aroma transect extends from the western side of the Andean Precordillera towards the Central Depression of the Atacama Desert (19°46'53.1"S, 69°40'02.4"W;

19°31'42.7"S, 69°22'43.2"W; Fig. 1). The elevation decreases from the Andes towards the Central Depression, from about 2700 to 1300 m.a.s.l., following an increase of aridity.

The Aroma transect is devoid of any vegetation due to the low amount of annual precipitation, which ranges from 26 mm $year^{-1}$ at Ar2720 to 5 mm $year^{-1}$ at Ar1340 (Houston, 2006) (Table S1). Annual plants grow with sufficient rainfall at higher elevations. The underlying parent material of the study area mainly consists of alluvial sediments of the El Diablo Formation (Pinto et al., 2004). The upper member of the El Diablo Formation covers the surface of the Aroma transect and consists of gravels and conglomerates of igneous origin from the Oligo-Miocene and Paleocene (basalt–andesite) (Pinto et al., 2004). The surface is covered by a well-developed desert pavement with a mostly homogenous mosaic of clasts. Due to long-term absence of surface activity or run-off, atmospheric deposition of gypsum and other soluble evaporites led to the evolution of a gypsum soil cover. Thus, soils of the Aroma transect are weak to moderately alkaline (Table S1). Wang et al. (2015) calculated gypsum soil formation and deposition ages using meteoric ^{10}Be in the Central Valley, and revealed the buildup of 2.25 m soil during the past ~6.6 Ma. The formation of the top10 cm soil was estimated to have occurred during the past ~0.29 Ma.

Samples were taken in February 2014, from five elevations (2720, 2455, 2020, 1680 and 1340 m.a.s.l.) (Fig.1), and from three depths (0-1, 1-5 and 5-10 cm). This strategy was chosen to separate surface crust from underlying layers, assuming the surface layer protects subsoils against wind erosion (Ewing et al., 2006). All sampling sites were completely devoid of plants at the time of sampling.

In addition, samples (depths of 0-1, 1-5 and 5-10 cm) were collected at Yungay, located southeast of Antofagasta (Chile), around 60 km from the coast and at an elevation of about 1000 m.a.s.l., with a mean precipitation between 2-5mm yr^{-1} (Houston, 2006). Due to the low

precipitation, this site lacks vegetation. However, incidental evidence of microbial life has been found in the soils of Yungay (Navarro-González et al., 2003; Connon et al., 2007; Schulze-Makuch et al., 2018).

2.2. Sequential P fractionation

Soil P concentrations were determined by sequential P fractionation (Hedley et al., 1982; Tiessen and Moir, 1993), which could provide information on its potential availability. Four reagents (anion exchange resin, 0.5M $NaHCO_3$, 0.1M NaOH and 1M HCl) were used successively to extract phosphate from 0.5 g of air-dried soil, and finally, residual P was extracted by *aqua regia* digestion at 130ºC. The concentration of inorganic P in the extracted solutions was determined by the malachite green method (Ohno and Zibilske, 1991) and measured at 630 nm by a microplate reader (Tecan infinite M200pro spectrophotometer Groedig, Austria), total P (P_t) was determined by ICP-OES (ICP–OES; Ultima 2, HORIBA Jobin Yvon, Longjumeau, France), and organic P (P_o) was calculated as the difference between P_t and P_i.

2.3. Oxygen isotope composition of HCl-extractable P_i

The preparation of silver phosphate for measuring $\delta^{18}O_{HCl\text{-}P}$ required first the extraction of phosphate from soil samples and then purification. Air-dried soils (20 g) were successively extracted by 0.5M $NaHCO_3$ and 0.1M NaOH (1:10 soil: solution ratio) before a final extraction with 1M HCl. The alkaline extracts were discarded, and only the 1M HCl extract was used for the purification of phosphate (Amelung et al. 2015). The extracted phosphate was purified using the method developed by Tamburini et al. (2010). This was done by successive precipitation of phosphate as ammonium phosphomolybdate and then as magnesium ammonium phosphate. After this last precipitation step, the crystals were dissolved, the solution cleaned with a cation exchange resin and the remaining phosphate was precipitated as silver phosphate (Ag_3PO_4). Two of the

samples with the highest content of HCl-P_o were additionally extracted with ^{18}O-labeled 1M HCl solution to detect the potential incorporation of oxygen from the reagent via inorganic hydrolysis of organic compounds and/or condensed phosphate. The $\delta^{18}O$ value of silver phosphate (two replicates of the same sample) was measured by the Plant Nutrition group at ETH Zurich using a Vario PYRO Cube (Elementar, Hanau, Germany) in pyrolysis mode, coupled in continuous flow to an Isoprime 100 isotope ratio mass spectrometer (Isoprime, Manchester, UK). $\delta^{18}O$ values are reported in the conventional δ notation relative to Vienna Standard Mean Ocean Water (VSMOW). Calibration of results was done by using an internal Ag_3PO_4 standard ($\delta^{18}O$ = 14.2‰) and two international benzoic acid standards, IAEA 601 ($\delta^{18}O$ = +23.3‰) and IAEA 602 ($\delta^{18}O$ = +71.4‰) distributed by the International Atomic Energy Agency, Vienna, Austria. Standard deviation of replicate analysis of standards was ± 0.4‰.

The empirical equation of Chang and Blake (2015) was used to calculate the equilibrium range of $\delta^{18}O_p$, where T is the ambient temperature in K, and $\delta^{18}O_p$ and $\delta^{18}O_{sw}$ are $\delta^{18}O$ values of phosphate and ambient soil water in ‰, respectively:

$$\delta\,^{18}O_p = e^{\left(\frac{14.43}{T_{soil}} - \frac{26.54}{1000}\right)} \times (\delta\,^{18}O_{sw} + 1000) - 1000 \qquad [1]$$

The annual air temperature (T_{air}) was estimated by an empirical linear regression between elevation and temperature as developed by the Chilean Ministry of Public Affairs (Amphos 21 Consulting Chile, 2013), which is based on the interpolation of data from adjacent weather stations (Table S1). Estimation of the annual soil temperature (T_{soil}) was done using the data from two weather stations (Collaborative Research Center 1211, Hoffmeister, 2017) located approximately at the beginning (1366 m, 19°45'40"S, 69°39'18"W) and end (2639 m, 19°31'44"S, 69°23'31"W) of the Aroma transect. The difference between the annual soil and air temperature was 5.1 and 4.1°C in stations 1366 and 2639 m, respectively. The mean of these values, 4.6°C, was used to

estimate the soil temperature at the depth of 0-1 cm and 1-5 cm. Moreover, the annual soil temperature at the depth of 10 cm was 2.0 and 4.1°C higher than the surface soil, respectively, resulting in an increase of 3.1°C averagely to assess soil temperature for the 5-10 cm soil horizon. Although the ^{18}O of rainwater varied between -11‰ and -1‰ from an extreme rainfall event in the Atacama Desert (Jordan et al., 2019), the $\delta^{18}O$ of precipitation at our sampling sites, which is within 50 kilometers from Ar1340 to Ar2720 (Fig. 1), is about -7.0 ‰ according to the published $\delta^{18}O$ values of modern precipitation at similar elevation to Aroma (Aravena et al., 1999; Boschetti et al., 2019). Thus, -7.0 ‰ was used as the lower $\delta^{18}O_{SW}$ extreme for the equilibrium calculation. An enrichment factor of 3‰ and 6‰ was also used to calculate the mean and the upper extreme (Rothfuss et al., 2015; Schulze-Makuch et al., 2018). Another method to determine the $\delta^{18}O_{SW}$ is the use of oxygen isotope composition of soil carbonate according to the equation of Kim and O'Neil (1997):

$$1000 \times ln\alpha_{(Carbonate-H2O)} = 18.03 \times \left(10^3 \times T_{soil}{}^{-1}\right) - 32.42 \quad [2]$$

where α is the fractionation factor between soil carbonate and soil water oxygen isotopes, and T is soil temperature in K. The fractionation factor α is related to δ as equation [3]:

$$\alpha_{(Carbonate-H2O)} = \frac{1000 + \delta_{carbonate}}{1000 + \delta_{H2O}} \quad [3]$$

According to the research by Quade et al. (2007), $\delta^{18}O$ of soil carbonate in the soil layer of 0-10 cm in Atacama Desert ranges from 30‰ to 32‰ at similar elevation to Aroma. Although the range of $\delta^{18}O$ in soil carbonate is limited by the amount of observed data, the calculated $\delta^{18}O_{sw}$ ranges from -1.0 to 1.1 ‰, which is closer to the measured values (-7.0 – -1.0 ‰). We therefore, calculated

the range of isotopic equilibrium between phosphate and water using the combined maximal possible range of $\delta^{18}O_{sw}$ from -7.0 to 1.1‰.

2.4. Isotopic equilibrium and contribution of biological P cycling in HCl-extractable P_i

Based on the equation proposed by Gross and Angert (2015), the contribution of biological P cycling in HCl-P pool (%) was calculated based on the $\delta^{18}O_P$ values of the parent material [$\delta^{18}O_{P\ (parent\ material)}$], the soil HCl-P pool [$\delta^{18}O_{P\ (HCl\text{-}P\ pool)}$], and the isotopic equilibrium value [$\delta^{18}O_{P\ (equilibrium)}$] in a mass-balance approach as:

$$P_{(contribution\ by\ biological\ cycling)} = \frac{\delta\ ^{18}O_{p\ (HCl-P\ pool)} - \delta\ ^{18}O_{p\ (parent\ material)}}{\delta\ ^{18}O_{p\ (equilibrium)} - \delta\ ^{18}O_{p\ (parent\ material)}} \quad [4]$$

The $\delta^{18}O_P$ value of the parent material [$\delta^{18}O_{P\ (parent\ material)}$] is10 ± 0.9 ‰ in Aroma (Table S3). The average soil temperature across Aroma transect and Yungay is 12.5°C in the depths of 0-1 and 1-5 cm, and 15.6°C in the depth of 5-10 cm. The minimal, mean and maximal isotopic equilibrium values [$\delta^{18}O_{P\ (equilibrium)}$] were calculated following Eq. [1], resulting in 17.1‰, 20.2‰ and 25.4‰ for the soil depth of 0-1 and 1-5 cm, and 16.5‰, 19.6‰ and 24.8‰ for the soil depth of 5-10 cm, respectively.

3. RESULTS

3.1. Various P pools separated by sequential P fractionation

Inorganic P (P_i) dominated the overall composition of P pools (Fig. 2). Over 80% of the total P in the soils was HCl-extractable P. After that, residual P was the second largest P pool, contributing to about 8-23% of total P. The concentration of labile forms of P (resin and $NaHCO_3$ P) was low with a range of 7-67 mg kg^{-1} in all the samples, though slightly elevated in the less arid sites Ar2020 and Ar2720 at 5-10 cm depth. The distribution of P among the different pools at the

hyperarid Yungay was comparable at all three soil depths, and similar to the P distribution found in the driest site of the Aroma transect (Ar1340; Fig. 2).

3.2. Oxygen isotope composition of HCl-extractable P_i

We did not observe significant differences in $\delta^{18}O_{HCl\text{-}P}$ values between the same sample extracted by ^{18}O-labeled and unlabeled HCl solutions (Table S3). We therefore concluded that inorganic hydrolysis and oxygen incorporation was not occurring during soil P extraction. According to Eq. 1 and the $\delta^{18}O_{sw}$ range, the average minimum and maximum equilibrium $\delta^{18}O_{HCl\text{-}P}$ values of all sites among three soil layers were 16.5‰ and 25.4‰, respectively (Fig. 3; solid green lines). The $\delta^{18}O_{HCl\text{-}P}$ values at Yungay and at the driest site of Aroma (Ar1340) (Fig. 3) were in a similar range, and far away from the estimated range of isotopic equilibrium. At all sites, the surface soils (0-1cm) showed consistently the lowest $\delta^{18}O_{HCl\text{-}P}$ values, with a rising trend towards isotopic equilibrium with increasing soil depth (Fig. 3). Moreover, there was a considerable variation of $\delta^{18}O_{HCl\text{-}P}$ values in the upper soil layer, from 9.9‰ in the driest site to 12.2‰ in the wettest site. The variation was even larger in the deeper soil layers, with a variation of 6‰ and 13.8‰ in the second (1-5cm) and third (5-10cm) soil layer, respectively (Fig. 3). Hence, the degree of isotope exchange varied with soil depth and region.

4. DISCUSSION

4.1. Estimation of the oxygen isotope equilibrium

In order to interpret the measured $\delta^{18}O_{HCl\text{-}P}$ values, the oxygen isotope equilibrium has to be estimated based on the $\delta^{18}O_{sw}$ value and soil temperature according to the Eq.1. Soil water in the Atacama Desert is derived from sporadic rainfall and gypsum hydration water (Shen et al., 2020). However, rainwater is the dominate soil water resource at arid sites in the Atacama Desert, even

under conditions of less than 20 mm year^{-1} rainfall (Orlando et al. 2010; Schulze-Makuch et al. 2018). Thus, $\delta^{18}O_{SW}$ was mainly determined by rainwater rather than gypsum hydration water.

Previous studies on oxygen isotope composition of rainfall water revealed that $\delta^{18}O$ in rainwater was depleted in the high elevation area due to an altitude isotope effect when air masses ascend the Andes (Aravena et al., 1999; Boschetti et al., 2019; Shen et al., 2020). This effect is relatively weak between 2000 and 3000 m.a.s.l. in the Andes, whereas the $\delta^{18}O$ value in rainwater ($\delta^{18}O_w$) declines strongly above 3500 m.a.s.l. (Fritz et al., 1981). Boschetti et al. (2019) reported that the $\delta^{18}O_w$ value in the Andes' rainwater decreased from -7.13‰ (Alto Mocha, 19°45'5"S, 69°17'55"W) to -7.51‰ only (Chusmiza, 19°42'22"S, 69°11'26"W) when elevation increased from 2590 to 3360 m.a.s.l. Quade et al. (2007) showed that the $\delta^{18}O_w$ value in rainwater remained stable at -5.6‰ when elevation increased from 130 to 1460 m.a.s.l. in the Paposa transect, indicating that altitudinal effects on rainwater oxygen isotope composition is hardly pronounced at such low levels above the sea. Here, all our sampled sites are located below 3500 m.a.s.l., with a mean range a.s.l of 1340 to 2720 m. across a distance of 50 kilometers (Fig. 1). Therefore, we consider a value of -7‰ as a justified lower limit of $\delta^{18}O_w$ of rainwater at the Aroma transect, which was thus used to calculate the lower limit of the equilibrium range for soil phosphates according to Eq. 1, in accordance with the published $\delta^{18}O$ values of precipitation at similar elevation in the Atacama Desert (Aravena et al., 1999; Boschetti et al., 2019). Yet, once the rainwater enters to soil, it may evaporate, leaving more stable isotopes behind. We thus also had to calculate an upper limit for the $\delta^{18}O_w$ of soil pore water and thus the equilibrium range for soil phosphates.

At the arid sites, continuous evaporation during the long intervals between two rain events in dry areas may lead to significant oxygen isotope fractionation and consequent enrichment of heavier ^{18}O isotopes in soil water (Hsieh et al., 1998; Rothfuss et al., 2015; Schulze-Makuch et al.,

2018). The $\delta^{18}O_{SW}$ values thus generally increase from a minimum value at soil surface to a maximum value at the deepest part of the Evaporation Front (EF), from where they decrease exponentially with depth until reaching constant values at deeper soil layers (Allison et al., 1983). Rothfuss et al. (2015) showed that the EF could reach the depth of 6 cm in an initially saturated sand column after 290 days with a maximum stable ^{18}O-isotope enrichment of about 6‰ relative to the land surface. Ebeling et al. (2016) also observed an enrichment due to soil water evaporation in the $\delta^{18}O$ of soil water in the surface layers of a soil profile on a late Tertiary alluvial fan (located in the Atacama at ~ 28°10'), with an apparent enrichment of 3‰ to 4‰ compared to the $\delta^{18}O$ value in the rainfall water. Schulze-Makuch et al. (2018) measured the $\delta^{18}O_{SW}$ value at Yungay site (-1.95‰) one month after the exceptional rainfall in 2015 and found an enrichment of about 3‰ relative to the rainwater (~ -4.9‰ ± 1.1‰, calculated from the Bowen equation; Bowen and Revenaugh, 2003). They further measured $\delta^{18}O_{SW}$ values one year after the rain and found that $\delta^{18}O_{SW}$ was reset to that of rainwater. We thus consider a 6‰ enrichment factor which was also used to calculate the upper limit of the equilibrium window in order to cover the uncertainties of soil water enrichment over a larger timescale, and a stable-isotope enrichment by 3‰ as a reasonable enrichment factor for estimating the mean isotopic equilibrium value for each site. Meanwhile, a similar range of $\delta^{18}O_{SW}$ value (-1.0 to 1.1 ‰) was assessed according to the $\delta^{18}O$ in soil carbonate, resulting in a bit higher for the upper limit of the equilibrium. Therefore, 1.1 ‰ was used for the calculation of maximal isotopic equilibrium.

Indeed, the isotopic equilibrium range should cover values over a long period of time rather than just at the time of sampling. In the Atacama Desert, a precise reconstruction of the past temperature has so far been challenging due to the lack of a reliable long-term archive (Houston, 2002; Quade et al., 2007). In our study, air temperature ranged from 15.8 to 18.5°C at all research sites (Table

S1) and soil temperature in the depths of 0-1 and 1-5 cm was obtained by the mean of air temperature with subtraction of 4.6 °C, which was the difference between air and soil surface temperature observed in weather stations. Meanwhile, soil temperature in the depths of 5-10 cm was 3.1°C higher than the surface soil. Although they only have two years of data available, it still provides information on the estimation of equilibrium oxygen isotope fractionations in phosphate.

4.2. Interpretation of the measured $\delta^{18}O_{HCl\text{-}P}$ values

In biological systems, full oxygen isotope exchange between phosphate and water can happen very fast. Cell-free experiments with a higher concentration of pyrophosphatase than natural environments revealed that biologically-driven isotopic equilibrium could occur after one or two days (Blake et al., 2005; von Sperber et al., 2017). In the Atacama Desert and under dry conditions, microbial activity likely persists at a minimal level, but it quickly increases when water is abundant (Jones et al., 2018; Schulze-Makuch et al., 2018). This implies that the biological activity and thus cycling of P may take place rapidly after each rainfall event.

The $\delta^{18}O_P$ value of parent material in Aroma transect is around 10‰ (Table S3), resembling the $\delta^{18}O_P$ values of apatite in igneous rocks (6-8‰; Blake et al., 2010). The $\delta^{18}O_{HCl\text{-}P}$ values that are distant from the equilibrium range, such as Ar1340 and Ar2455 at 0-1 and 1-5 cm (Fig. 3), lack isotope effects of P cycling by biological processes (Tamburini et al., 2012; Helfenstein et al., 2018). Indeed, no more than 8% of HCl-P has been biologically cycled at 0-1 and 1-5 cm in Ar2455 as the estimated contribution of biological P cycling (Table 1). Previous studies have shown that fractionation by abiotic processes, like mineral precipitation, dissolution of apatite or adsorption-desorption reactions of phosphate, is small and does not exceed 1‰ (Liang and Blake, 2007; Jaisi et al., 2010). Despite contradictory opinions about the isotopic effect of abiotic processes between Jaisi et al. (2010) and Melby et al. (2013), these are small compared to biotic processes and cannot

cause large observed shifts of $\delta^{18}O_{HCl\text{-}P}$ values, as, e.g., observed for the increase in soil $\delta^{18}O_{HCl\text{-}P}$ values with depth at sites Ar2020 and Ar2720 (Fig. 3). This increase is also larger than that attributable to the evaporative enrichment of heavy oxygen at the soil surface (≤ 6‰; see above). Hence, this shift of $\delta^{18}O_{HCl\text{-}P}$ values towards isotopic equilibrium values indicates biological cycling of phosphates, and values within the isotopic equilibrium range indicate a complete oxygen isotope exchange between phosphate and ambient water.

Although soil labile P (resin P, $NaHCO_3$ P) concentrations in the Atacama Desert are lower in comparison with other ecosystems (Cross and Schlesinger, 1995), when microorganisms absorb P from labile pools, the metabolic pathways catalyzed by intracellular enzymes like inorganic pyrophosphatase lead to the temperature-dependent equilibrium between $\delta^{18}O_p$ and $\delta^{18}O_{SW}$ (Longinelli and Nuti, 1973; Blake et al., 2005; Tamburini et al., 2012). This biologically cycled P is then released after cell death and lysis (Tamburini et al., 2012). Over time, these phosphates can precipitate as secondary Ca-P minerals and, finally, overprint the $\delta^{18}O$ value of primary Ca-P minerals in the HCl-P pool (Joshi et al., 2016).

The long turnover time of the HCl-P pool allows to determine the soil biological mediated P cycling. In dry environments, primary P minerals can remain intact even after 150 kyr of soil development (Helfenstein et al., 2018). In a study by Tamburini et al., (2012) along a soil chronosequence with soil up to 3000 years of age, only the oldest soil had $\delta^{18}O_{HCl\text{-}P}$ values in the equilibrium range. Thus, in our study, the observed $\delta^{18}O_{HCl\text{-}P}$ values within the equilibrium range record the occurrence of biological activity during the rare periods when the water content in the soil was higher. The patchiness of $\delta^{18}O_{HCl\text{-}P}$ values along the gradient, being larger at site Ar2020 and Ar2720 than Ar1680 and Ar2455, reflects the spatial heterogeneity and uneven occurrence of life in the Atacama Desert (Navarro-González et al., 2003; Maier et al., 2004; Connon et al., 2007).

By using the $\delta^{18}O_P$ values of the parent material, the soil HCl-P pool, and the isotopic equilibrium value, we estimate that the amount of P in the HCl-P pool was biologically cycled at the different sites and depths, before being precipitated as Ca-P minerals. According to the calculation based on minimum and maximal isotopic equilibrium value, 1-31% of P in HCl-P pool (except site Ar1340) were estimated for biological cycling in 0-1cm soil depth; this portion rose to 4-86% at 1-5 cm depth, and more than 13% of biologically cycled P are found at 5-10 cm soil depth, respectively (Table 1; for calculations, see Equation 4). In general, the degree of biologically cycled P increased with soil depth (Table 1). This is valid at all sites, except site Ar1340, reflecting limited biological activity due to the least amount of rainfall. In contrast, past biological activity more or less accounted for full recycling of the soil HCl-P in 5-10 cm soil depth at higher rainfall sites of Ar2020 and Ar2720 (Table 1).

In principle, the input of phosphate via atmospheric deposition with higher $\delta^{18}O_p$ values (Gross et al., 2013) could potentially be a source of elevated $\delta^{18}O_p$, although this should have rather led to $\delta^{18}O_p$ maxima at the soil surface and not below it. However, several evidences indicate that this was not the case. First, according to the P concentrations in dust and the amount of dust via atmospheric deposition (Ewing et al., 2006; Mahowald et al., 2008), the P content in dust at these site of the Atacama Desert was less than 8 mg kg^{-1}, suggesting little impact from eolian sources on the $\delta^{18}O_P$ of the studies sites. Secondly, studies reported that according to sampled soils across the desert, the mineral particles from atmospheric deposition were composed of anorthite ($CaAl_2Si_2O_8$), calcium sulphate ($CaSO_4$), quartz (SiO_2), and albite ($NaAlSi_3O_8$) (Wang et al., 2014; 2015). Although this description cannot give any indication on the P content of the dust, the mineralogical assemblage (except $CaSO_4$, common in hyper arid regions) is characteristic of

igneous origin of the dust. In this case, we would expect low $\delta^{18}O_P$ values from the dust not high values (Mizota et al., 1992; Smith et al., 2021). About eolian contribution from sedimentary rocks, information on the P content of these formations is scarce, but it points to low P concentrations. Thirdly, $\delta^{18}O_{HCl\text{-}P}$ values did not show a regular trend along elevation in the Aroma transect, which also refused the P source via atmospheric deposition. In addition, a study by Pinto et al. (2004) revealed that marine sedimentary rocks in the Andes to the east of the Atacama Desert lacked phosphate, without giving any additional estimation. If outcropping Jurassic marine calcareous sediments from Coastal Cordillera are a source of high $\delta^{18}O_p$ values (Vásquez and Sepúlveda, 2013), then this should have led to higher $\delta^{18}O_p$ in the sites of lower elevations, which was not the case. Therefore, the shift of $\delta^{18}O_{HCl\text{-}P}$ values in the Atacama Desert most likely resulted from past biological activities following rainfall occurrence, and it could be used as evidence of biologically cycled P.

Knief et al. (2020) reported that soils of the Aroma transect contained up to 800 ng phospholipid fatty acids (PLFA) per gram soil. As there are different conversion factors in place to translate these values into microbial biomass, Willers et al. (2015) suggested to use the values directly as measures for living microbial biomass. Taking the most abundant PLFA C16:0 as reference, this means that we might expect about one third, i.e. approx. 270 ng of P in PLFA of living microbial cells. Phospholipids, together with nucleic acids are the dominant form of P, comprising of up to 60% of total microbial P (Vadstein, 2000; Buenemann et al., 2011). Concentrations of HCl-Pi were in the range of a several hundred µg Pi g^{-1} soil, i.e., larger by a factor of 1000. Even if only one tenth was, on average, biologically cycled, this is still two magnitudes larger than the amount that could potentially be stored in living microbial biomass (which usually also contains P_i in more easily extractable pool). Even if such gross calculations have many remaining uncertainties, the

different magnitudes provide a clear evidence, that our detected changes in $\delta^{18}O_p$ values do not reflect recent living biomass but a preservation of a signal across at least several centuries a tracing of past life. Quantifying the latter and their related turnover times might now warrant further attention.

5. CONCLUSIONS

The most hyper-arid sites in the Aroma and Yungay regions of the Atacama Desert showed little evidence of biological P. However, biological cycling of soil P did increase with decreasing aridity. Even though biological cycling has a relatively small share in the overall P cycling in this environment, it has a significant effect on the oxygen isotopic composition of phosphates, which was preserved in secondary minerals forming during the precipitation of secondary calcium phosphates. The $\delta^{18}O$ in phosphate is therefore a powerful tool to trace past biological activity in the Atacama Desert, which approaches the dry limit on Earth for various forms of life. Given the extreme environment of the Atacama desert, this method could possibly be used to trace evidence of life in other extreme terrestrial and extraterrestrial environments, such as Mars.

ACKNOWLEDGMENTS

This work was done as part of a Collaborative Research Center project CRC1211: 'Earth-Evolution at the Dry Limit,' funded by the Deutsche Forschungsgemeinschaft (DFG, German Research Foundation) – Projektnummer 268236062 – SFB 1211. Ye Wang would like to thank the China Scholarship Council for the financial support (No. 201606040185).

REFERENCES

Allison G.B., Barnes C.J., Hughes M.W. (1983) The distribution of deuterium and 18O in dry soils 2. Experimental. *J. Hydrol.* **64**, 377-397.

Amelung W., Antar P., Kleeberg I., Oelmann Y., Lücke A., Alt, F. et al. (2015) The $\delta^{18}O$ signatures of HCl-extractable soil phosphates: methodological challenges and evidence of the cycling of biological P in arable soil. *Eur. J. Soil Sci.* **66**, 965-972.

Amphos 21 Consulting Chile, L. (2013) Analisis de Los Recursos Hidricos de La Quebrada de Aroma, Region de Tarapaca, Technical Report, Ministerio de Obras Publicas, www.repositoriodirplan.cl:443/xmlui/handle/20.500.12140/25865

Anderson K., Wells S., Graham R. (2002) Pedogenesis of vesicular horizons, Cima Volcanic Field, Mojave Desert, California. *Soil Sci. Soc. Am. J.* **66**, 878-887.

Aravena R., Suzuki O., Pena H., Pollastri A., Fuenzalida H., Grilli A. (1999) Isotopic composition and origin of the precipitation in Northern Chile. *Appl. Geochemistry* **14**, 411-422.

Bauke S.L., von Sperber C., Siebers N., Tamburini F., Amelung W. (2017) Biopore effects on phosphorus biogeochemistry in subsoils. *Soil Biol. Biochem.* **111**, 157-165.

Blake R.E., Alt J.C., Martini A. M. (2001) Oxygen isotope ratios of PO_4: An inorganic indicator of enzymatic activity and P metabolism and a new biomarker in the search for life. *Proc. Natl. Acad. Sci.* **98**, 2148-2153.

Blake R.E., O'Neil J.R., Surkov A.V. (2005) Biogeochemical cycling of phosphorus: Insights from oxygen isotope effects of phosphoenzymes. *Am. J. Sci.* **305**. 596-620.

Blake R.E., Chang S.J., Lepland A. (2010) Phosphate oxygen isotopic evidence for a temperate and biologically active Archaean ocean. *Nature* **464**, 1029-1032.

Boschetti T., Cifuentes J., Lacumin P., Selmo E. (2019) Local meteoric water line of Northern Chile (18° S-30° S): An application of error-in-variables regression to the oxygen and hydrogen stable isotope ratio of precipitation. *Water* **11**, 791.

Bowen G.J., Revenaugh J. (2003) Interpolating the Isotopic Composition of Modern Meteoric Precipitation. *Water Resour. Res.* **39**. 10.

Buenemann E.K., Prusisz B., Ehlers K. (2011) Characterization of Phosphorus Forms in Soil Microorganisms, in: Bünemann, E., Oberson, A., Frossard, E. (Eds.), Phosphorus in Action: Biological Processes in Soil Phosphorus Cycling, Soil Biology. Springer, Berlin, Heidelberg, pp. 37-57.

Chang S.J., Blake R.E. (2015) Precise calibration of equilibrium oxygen isotope fractionations between dissolved phosphate and water from 3 to 37°C. *Geochim. Cosmochim. Acta* **150**, 314-329.

Connon S.A., Lester E.D., Shafaat H.S., Obenhuber D. C., Ponce A. (2007) Bacterial Diversity in Hyperarid Atacama Desert Soils. *J. Geophys. Res. Biogeosciences* **112**, G04S17.

Cross A.F., Schlesinger W.H. (1995) A literature review and evaluation of the Hedley fractionation: Applications to the biogeochemical cycle of soil phosphorus in natural ecosystems. *Geoderma* **64**, 197-214.

Dunai T.J., Lopez G.A.G., Juez-Larre J. (2005) Oligocene-Miocene age of aridity in the Atacama Desert revealed by exposure dating of erosion-sensitive landforms. *Geology* **33**, 321-324.

Dunai T., Melles M., Quandt D., Knief C., Amelung W. (2020) Whitepaper: Earth – Evolution at the dry limit. *Glob. Planet. Change* **193**, 103275.

Ebeling A., Oerter E., Valley J.W., Amundson R. (2016) Relict soil evidence for profound quaternary aridification of the Atacama Desert, Chile. *Geoderma* **267**, 196-206.

Evenstar L.A., Hartley A.J., Stuart F.M., Mather A.E., Rice C.M., Chong G. (2009) Multiphase development of the Atacama Planation Surface recorded by cosmogenic ^{3}He exposure ages: implications for uplift and Cenozoic climate change in western South America. *Geology* **37**, 27-30.

Ewing S.A., Sutter B., Owen J., Nishiizumi K., Sharp W., et al. (2006) A threshold in soil formation at Earth's arid-hyperarid transition. *Geochim. Cosmochim. Acta*, **70**, 5293-5322.

Fritz P., Suzuki O., Silva C., Salati E. (1981) Isotope hydrology of ground waters in the Pampa del Tamarugal, Chile. *J. Hydrol.* **53**, 161-184.

Gérard F. (2016) Clay minerals, iron/aluminum oxides, and their contribution to phosphate sorption in soils: A myth revisited. *Geoderma* **262**, 213-226.

Gross A., Angert A. (2015) What processes control the oxygen isotopes of soil bioavailable phosphate? *Geochim. Cosmochim. Acta* **159**, 100-111.

Gross A., Nishri A., Angert A. (2013) Use of phosphate oxygen isotopes for identifying atmospheric-P Sources: A case study at Lake Kinneret. *Environ. Sci. Technol.* **47**, 2721-2727.

Helfenstein J., Tamburini F., von Sperber C., Massey M.S., Pistocchi C., Chadwick O.A., Vitousek P.M., Kretzschmar R., Frossard E. (2018) Combining spectroscopic and isotopic techniques gives a dynamic view of phosphorus cycling in soil. *Nat. Commun.* **9**, 3226.

Hartley A.J., Chong G. (2002) Late Pliocene age for the Atacama Desert: implications for the desertification of western South America. *Geology* **30**, 43-46.

Hartley A.J., Chong G., Houston J., Mather A.E. (2005) 150 million years of climatic stability: evidence from the Atacama Desert, northern Chile. *J. Geol. Soc.* **162**, 421-424.

Hedley M.J., Stewart J.W.B., Chauhan B.S. (1982) Changes in inorganic and organic soil phosphorus fractions induced by cultivation practices and by laboratory incubations. *Soil Sci. Soc. Am. J.* **46**, 970-976.

Hoffmeister D. (2017). Collaborative research center 1211 – database. URI, http://www.crc1211db.uni-koeln.de/

Houston J. (2002) Groundwater recharge through an alluvial fan in the Atacama Desert, northern Chile: mechanisms, magnitudes and causes. *Hydrol. Process.* **16**, 3019-3035.

Houston J. (2006) Variability of precipitation in the Atacama Desert: its causes and hydrological impact. *Intern. J. Climatol.* **26**, 2181-2198.

Houston J., Hartley A.J. (2003) The central Andean west-slope rainshadow and its potential contribution to the origin of hyper-aridity in the Atacama Desert. *Intern. J. Climatol.* **23**, 1453-1464.

Hsieh J.C.C., Chadwick O.A., Kelly E.F., Savin S.M. (1998) Oxygen isotopic composition of soil water: Quantifying evaporation and transpiration. *Geoderma* **82**, 269-293.

Jaisi D.P., Blake R.E., Kukkadapu R.K. (2010) Fractionation of oxygen isotopes in phosphate during its interactions with iron oxides. *Geochim. Cosmochim. Acta* **74**, 1309-1319.

Jordan T.E., Herrera C., Godfrey L.V., Colucci S.J., Gamboa C., Urrutia J., Gonzalez G., Paul J.F. (2019) Isotopic characteristics and paleoclimate implications of the extreme precipitation event of March 2015 in northern Chile. *Andean Geol.* **46**, 1-31.

Jordan T.E., Kirk-Lawlor N.E., Blanco N., Rech J.A., Cosentino N.J. (2014) Landscape modification in response to repeated onset of hyperarid paleoclimate states since 14 Ma, Atacama Desert, Chile. *Geo. Soc. America Bulletin* **126**, 1016-1046.

Jones D. L., Olivera-Ardid S., Klumpp E., Knief C., Hill P. W., Lehndorff E., Bol R. (2018) Moisture Activation and Carbon Use Efficiency of Soil Microbial Communities along an Aridity Gradient in the Atacama Desert. *Soil Biol. Biochem.* **117**, 68-71.

Joshi S.R., Li X., Jaisi D.P. (2016) Transformation of phosphorus pools in an agricultural soil: An application of oxygen-18 labeling in phosphate. *Soil Sci. Soc. Am. J.* **80**, 69-78.

Kim S., O'Neil J. (1997) Equilibrium and noneequilibrium oxygen isotope effects in synthetic carbonates. *Geochim. Cosmochim. Acta* **61**, 3461-3475.

Knief C., Bol R., Amelung W., Kusch S., Frindte K., et al. (2020) Tracing elevational changes in microbial life and organic carbon sources in soils of the Atacama Desert. *Glob. Planet. Change* **184**, 103078.

Latorre C., Betancourt J.L., Arroyo M.T.K. (2006) Late Quaternary vegetation and climate history of a perennial river canyon in the Rio Salado basin (22 °S) of Northern Chile. *Quaternary Res.* **65**. 450-466.

Liang Y., Blake R.E. (2006) Oxygen isotope signature of Pi regeneration from organic compounds by phosphomonoesterases and photooxidation. *Geochim. Cosmochim. Acta* **70**, 3957-3969.

Liang Y., Blake R.E. (2007) Oxygen isotope fractionation between apatite and aqueous-phase phosphate: 20–45 °C. *Chem. Geol.* **238**, 121-133.

Liang Y., Blake R.E. (2009) Compound- and enzyme-specific phosphodiester hydrolysis mechanisms revealed by $\delta^{18}O$ of dissolved inorganic phosphate: Implications for marine P cycling. *Geochim. Cosmochim. Acta* **73**, 3782-3794.

Longinelli A., Nuti S. (1973) Revised phosphate-water isotopic temperature scale. *Earth Planet. Sci. Lett.* **19**, 373-376.

Maier R.M., Drees K.P., Neilson J.W., Henderson D.A., Quade J., Betancourt J.L. (2004) Microbial Life in the Atacama Desert. *Science* **306**, 1289-1290.

Mahowald N., Jickells T.D., Baker A.R., Artaxo P., Benitez-Nelson C.R., et al. (2008) Global distribution of atmospheric phosphorus sources, concentrations and deposition rates, and anthropogenic impacts. *Global Biogeochem. Cycles* **22**, GB4026.

Melby E.S., Soldat D.J., Barak P. (2013) Biological decay of 18O-labeled phosphate in soils. *Soil Biol. Biochem.* **63**, 124-128.

Mizota C., Domon Y., Yoshida N. (1992) Oxygen isotope composition of natural phosphates from volcanic ash soils of the Great Rift Valley of Africa and east Java, Indonesia. *Geoderma* **53**, 111-123.

Morgan A.M., Howard A.D., Hobley D.E.J., Moore J.M., Dietrich W.E., Williams R.M.E., Burr D.M., Grant J.A., Wilson S.A., Matsubara Y. (2014) Sedimentology and Climatic Environment of Alluvial Fans in the Martian Saheki Crater and a Comparison with Terrestrial Fans in the Atacama Desert. *Icarus* **229**, 131-156.

Navarro-González R., Rainey F.A., Molina P., Bagaley D.R., Hollen B.J. et al. (2003) Mars-like soils in the Atacama Desert, Chile, and the dry limit of microbial life. *Science* **302**, 1018-1021.

Nester P.L., Gayo E., Latorre C., Jordan T.E., Blanco N. (2007) Perennial stream discharge in the hyperarid Atacama Desert of northern Chile during the latest Pleistocene. *Proc. Nat. Acad. Sci.* **104**, 19724-19729

Nishiizumi K., Caffee M.W., Finkel R.C., Brimhall G., Mote T. (2005) Remnants of a fossil alluvial fan landscape of Miocene age in the Atacama Desert of northern Chile using cosmogenic nuclide exposure age dating. *Earth Planet. Sci. Lett.* **237**, 499-507.

Ohno T., Zibilske L.M. (1991). Determination of Low Concentrations of Phosphorus in Soil Extracts Using Malachite Green. *Soil Sci. Soc. Am. J.* **55**, 892-895.

Orlando J., Alfaro M., Bravo L., Guevara R., Caru M. (2010) Bacterial diversity and occurrence of ammonia-oxidizing bacteria in the Atacama Desert soil during a “desert bloom” event. *Soil Biol. Biochem*. **42**, 1183-1188.

Pinto L., Hérail G., Moine B., Fontan F., Charrier R., Dupré B. (2004) Using geochemistry to establish the igneous provenances of the Neogene continental sedimentary rocks in the Central Depression and Altiplano, Central Andes. *Sediment. Geol.* **166**, 157-183.

Pinto R., Barria I., Marquet P.A. (2006) Geographical distribution of *Tillandsia* lomas in the Atacama Desert, northern Chile. *J. Arid Environ.* **65**, 543-552.

Quade J., Rech J.A., Betancourt J., Latorre C., Quade B., et al. (2008) Paleowetlands and regional climate change in the central Atacama Desert, northern Chile. *Quat. Res.* **69**, 343-360

Quade J., Rech J.A., Latorre C., Betancourt J., Gleeson E., Kalin M.T.K. (2007) Soils at the hyperarid margin: The isotopic composition of soil carbonate from the Atacama Desert, Northern Chile. *Geochim. Cosmochim. Acta*. **71**, 3772-3795.

Rech J.A., Currie B.S., Michalski G., Cowan A.M. (2006) Neogene climate change and uplift in the Atacama Desert, Chile. *Geology* **34**, 761-764.

Rech J.A., Quade J., Hart W.S. (2003) Isotopic evidence for the source of Ca and S in soil gypsum, anhydrite and calcite in the Atacama Desert, Chile. *Geochim. Cosmochim. Acta*. **67**, 575-586.

Ritter B. Stuart F.M., Binnie S.A., Gerdes A., Wennrich V., Dunai T. (2018) Neogene fluvial landscape evolution in the hyperarid core of the Atacama Desert. *Sci. Rep.* **8**, 13952.

Rothfuss Y., Merz S., Vanderborght J., Hermes N., Weuthen A., Pohlmeier A., Vereecken H., Brüggemann N. (2015) Long-term and high-frequency non-destructive monitoring of water stable isotope profiles in an evaporating soil column. *Hydrol. Earth Syst. Sci*. **19**, 4067-4080.

Schulze-Makuch D., Wagner D., Kounaves S.P., Mangelsdorf K., Devine K.G., de Vera J.-P., Schmitt-Kopplin P., Grossart H.-P., Parro V., Kaupenjohann M., et al. (2018) Transitory microbial habitat in the hyperarid Atacama Desert. *Proc. Natl. Acad. Sci.* **115**, 2670-2675.

Shen J.X., Smith A.C., Claire M.W., Zerkle A.L. (2020) Unraveling biogeochemical phosphorus dynamics in hyperarid Mars-analogue soils using stable oxygen isotopes in phosphate. *Geobiology* **18**, 760-779.

Smith A.C., Pfahler V., Tamburini F., Blackwell M.S.A., Granger S.J. (2021) A review of phosphate oxygen isotope values in global bedrocks: Characterising a critical endmember to the soil phosphorus system. *J. Plant Nutr. Soil Sci.* **184**, 25-34.

Tamburini F., Bernasconi S.M., Angert A., Weiner T., Frossard E. (2010) A method for the analysis of the $\delta^{18}O$ of inorganic phosphate extracted from soils with HCl. *Eur. J. Soil Sci.* **61**, 1025-1032.

Tamburini F., Pfahler V., Bunemann E.K., Guelland K., Bernasconi S.M., Frossard E. (2012) Oxygen isotopes unravel the role of microorganisms in phosphate cycling in soils. *Environ. Sci. Technol.* **46**, 5956-5962.Tiessen H., Moir J. (1993) Characterization of available P by sequential extraction. In: Soil Sampling and Methods of Analysis (eds M.R. Carter and E.G. Gregorich), pp. 75-86. Lewis Publisher, Boca Raton, FL.

Vadstein O., (2000) Heterotrophic, Planktonic Bacteria and Cycling of Phosphorus, in: Schink, B. (Ed.), Advances in Microbial Ecology, Advances in Microbial Ecology. Springer US, Boston, MA, pp. 115 - 167.

Vásquez P., Sepúlveda F., (2013) Carats Iquique y Pozo Almonte, Región de Tarapacá. Servicio Nacional de Geología y Minería, Carta Geológica de Chile, Serie Geológica Básica, Nos. 162-163, mapa escala 1:100.000, Santiago, ISSN 0717-7283

von Sperber C., Kries H., Tamburini F., Bernasconi S.M., Frossard E. (2014) The effect of phosphomonoesterases on the oxygen isotope composition of phosphate. *Geochim. Cosmochim. Acta* **125**, 519-527.

von Sperber C., Tamburini F., Brunner B., Bernasconi S.M., Frossard E. (2015): The oxygen isotope composition of phosphate released from phytic acid by the activity of wheat and *Aspergillus niger* phytase. *Biogeosciences* **12**, 4175-4184.

von Sperber C., Lewandowski H., Tamburini F., Bernasconi S.M., Amelung W., Frossard E. (2017) Kinetics of enzyme-catalysed oxygen isotope exchange between phosphate and water revealed by Raman spectroscopy: kinetics of enzyme-catalysed oxygen isotope exchange. *J. Raman Spectrosc.* **48**, 368-373.

Wang F., Michalski G., Seo J.H., Ge W.S. (2014) Geochemical, isotopic, and mineralogical constraints on atmospheric deposition in the hyper-arid Atacama Desert, Chile. *Geochim. Cosmochim. Acta* **135**, 29-48.

Wang F., Michalski G., Seo J. H., Granger D. E., Lifton N., Caffee M. (2015). Beryllium-10 concentrations in the hyper-arid soils in the Atacama Desert, Chile: Implications for arid soil formation rates and El Niño driven changes in Pliocene precipitation. *Geochim. Cosmochim. Acta* **160**, 227-242.

Warren-Rhodes K.A., Rhodes K.L., Pointing S.B., Ewing S.A., Lacap D. et al. (2006) Hypolithic cyanobacteria, dry limit of photosynthesis, and microbial ecology in the hyperarid Atacama Desert. *Microb. Ecol.* **52**, 389-398.

Willers C., Jansen van Rensburg P.J., Claassens S. (2015) Phospholipid fatty acid profiling of microbial communities – a review of interpretations and recent applications. *J. Appl. Microbiol.* **119**, 1207-1218.

Figure captions

Fig. 1- (A) Colour shaded digital elevation model (Derived from SRTM-data, created using ArcGIS 10.5.1) with precipitation isoheyts (dashed black lines, Houston et al. 2006). Black line indicates the border between summer- and winter-rain dominated areas. The location of sampling sites at Yungay and along the Aroma aridity gradient in Chile are marked in red. (B) Satellite image (Google-Earth) indicating elevations of the Aroma transect (red circles), which decrease from the Andes towards the Central Depression, from 2720 to 1340 m.a.s.l.

Fig. 2- Concentration of different P pools extracted by sequential P extraction in mg kg^{-1}.

Fig. 3- $\delta^{18}O_{HCl\text{-}P}$ values in the three depth intervals and theoretical equilibrium calculated by annual mean soil temperature. The minimal and maximal equilibrium (solid green line) are calculated by $\delta^{18}O$ of rainwater estimated as -7‰ (Aravena et al., 1999; Boschetti et al., 2019) and 1.1‰ for the upper limit. Red line is the $\delta^{18}O_P$ value of bedrock in Aroma. Error bars represent the standard deviation of the mean (n=2).

Table 1- The percentage of biological cycling P in HCl-P pool was calculated based on $\delta^{18}O_P$ values of the parent material, the soil HCl-P pool, and the isotopic equilibrium value, including the minimal, mean, and maximal isotopic equilibrium values.

Site	Sampling depth	$\delta^{18}O_{HCl\text{-}P}$	Biological cycled P in HCl-P pool (minimal isotopic equilibrium value)	Biological cycled P in HCl-P pool (mean isotopic equilibrium value)	Biological cycled P in HCl-P pool (maximal isotopic equilibrium value)
	cm	‰	%	%	%
Ar1340	0-1	10.0	-	-	-
	1-5	10.1	-	-	-
	5-10	10.0	-	-	-
Ar1680	0-1	11.5	21.1	14.8	9.74
	1-5	13.9	55.0	38.4	25.32
	5-10	12.4	35.9	24.4	15.84
Ar2020	0-1	11.4	19.0	13.3	8.77
	1-5	15.9	82.4	57.5	37.99
	5-10	23.8	100.0*	100.0*	92.99
Ar2455	0-1	10.2	2.8	2.0	1.30
	1-5	10.6	7.8	5.4	3.57
	5-10	11.9	29.0	19.8	12.80
Ar2720	0-1	12.2	31.0	21.6	14.29
	1-5	16.1	86.0	60.0	39.61
	5-10	22.5	100.0*	100.0*	84.23

Ar1340 cannot be calculated due to its $\delta^{18}O_{HCl\text{-}P}$ values are close to the $\delta^{18}O_P$ value of the parent material.

**When the percentage of biological cycling P is larger than 100%, it is replaced by 100%.*

Fig.1.pdf

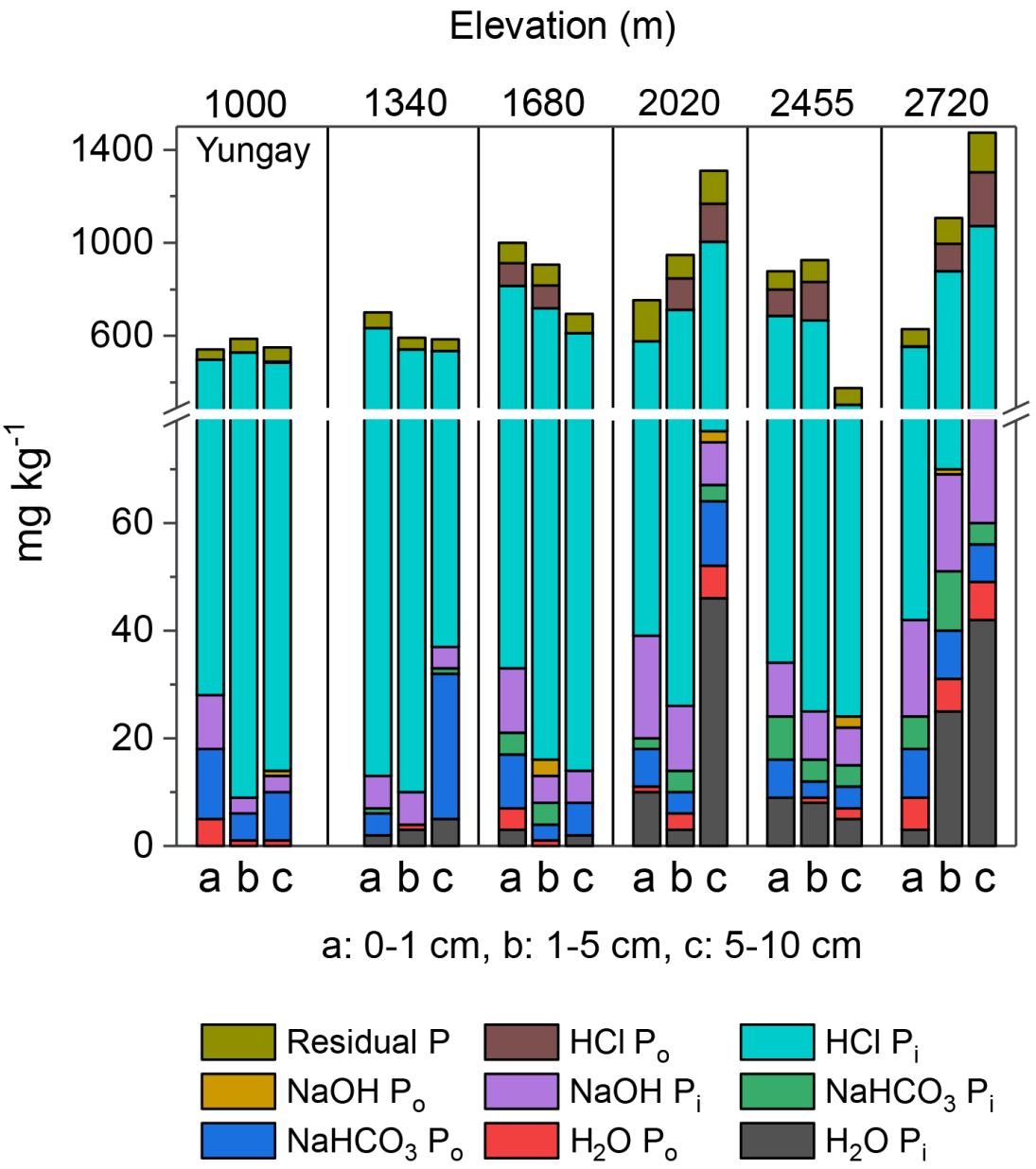
Elevation (m)
1000
1340
1680
2020
2455
2720
Yungay
1400
1000
600
60
40
20
0
mg kg-1
a b c
a: 0-1 cm, b: 1-5 cm, c: 5-10 cm
Residual P
HCl Po
HCl Pi
NaOH Po
NaOH Pi
NaHCO3 Pi
NaHCO3 Po
H2O Po
H2O Pi

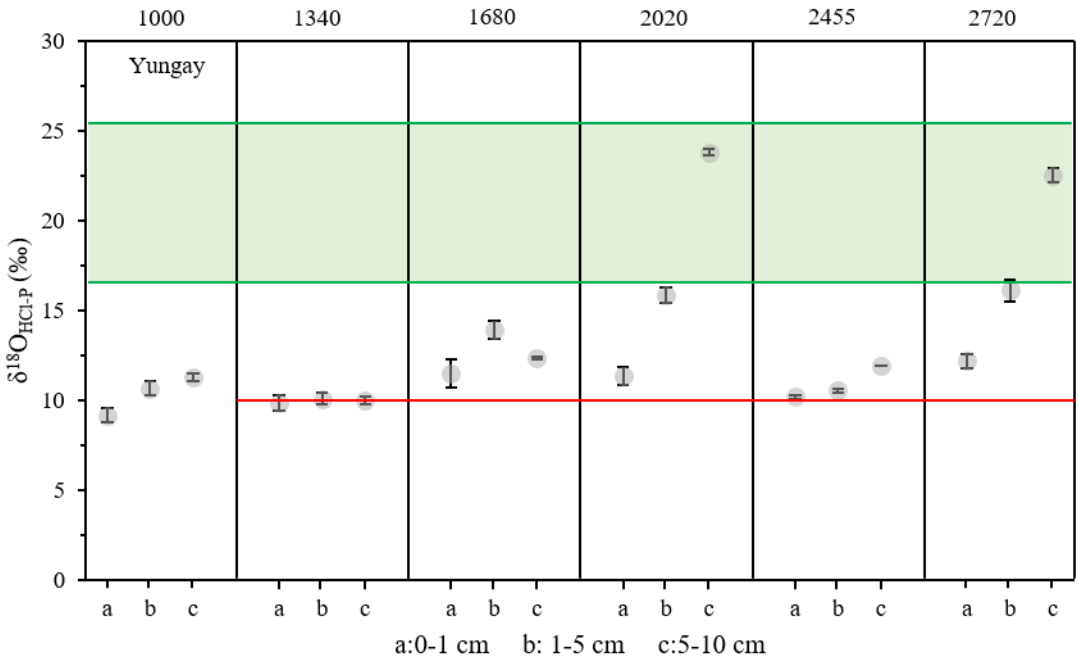
1000
1340
1680
2020
2455
2720
Yungay
30
25
20
15
10
5
0
$\delta^{18}O_{HCl-P}$ (‰)
a b c
a:0-1 cm b: 1-5 cm c:5-10 cm

Supplementary information for

Phosphate Oxygen Isotope Fingerprints of Past Biological Activity in the Atacama Desert

Table S1. The elevation, mean annual temperature, mean annual rainfall, calculated minimum and maximum equilibrium $\delta^{18}O_P$ values, and soil pH for all sampling sites.

Site	Geographic location	Elevation (m.a.s.l.)	Soil bulk density* (g cm^{-3})	Mean annual temperature (°C)	Mean annual rainfall (mm $year^{-1}$)	Minimum equilibrium (‰)	Maximum equilibrium (‰)	Sampling depth (cm)	Soil pH
Ar1340	19°46'53.1" S 69°40'02.4" W	1340	1.08	18.5	5	16.30	25.14	0-1 1-5 5-10	7.9 8.1 8.4
Ar1680	19°39'18.6" S 69°35'31.5" W	1680	1.32	18.2	7.5	16.35	25.19	0-1 1-5 5-10	7.8 8.0 8.3
Ar2020	19°35'44.8" S 69°30'26.8" W	2020	1.64	17.7	11.3	16.44	25.28	0-1 1-5 5-10	7.7 8.5 8.4
Ar2455	19°33'02.0" S 69°25'38.5" W	2455	1.80	16.6	19	16.63	25.48	0-1 1-5 5-10	7.6 7.9 8.3
Ar2720	19°31'42.7" S 69°22'43.2" W	2720	2.08	15.8	26.1	16.77	25.63	0-1 1-5 5-10	7.5

Yungay	24°06'06.1" S 70°01'05.8" W	1000	2.32	15.7	3.3	16.79	25.65	0-1 1-5 5-10	8.1 8.8 7.6 8.2 8.2

**Soil bulk density refers to the depth of 0-15cm, which cited from Moerchen et al. (2019).*

Mean annual Rainfalls are calculated by the equation of Houston (2006).

Mean annual temperatures are calculated by an empirical linear regression between elevation and temperature developed by the Chilean Ministry of Public Affairs (Amphos 21 Consulting Chile, 2013).

Table S2. Phosphorus concentrations of Hedley P fractionations for all sampling sites.

Site	Sampling depth	H_2O P_i	H_2O P_o	$NaHCO_3$ P_i	$NaHCO_3$ P_o	NaOH P_i	NaOH P_o	HCl P_i	HCl P_o	Residual P
	cm					mg kg^{-1}				
	0-1	2	0	4	1	6	0	621	0	68
Ar1340	1-5	3	1	0	0	6	0	531	0	51
	5-10	5	0	27	1	4	0	499	0	50
	0-1	3	4	10	4	12	0	781	100	87
Ar1680	1-5	0	1	3	4	5	3	702	99	90
	5-10	2	0	6	0	6	0	597	0	83
	0-1	10	1	7	2	19	0	538	0	177
Ar2020	1-5	3	3	4	4	12	0	687	134	100
	5-10	46	6	12	3	8	2	928	164	141
	0-1	9	0	7	8	10	0	651	115	79
Ar2455	1-5	8	1	3	4	9	0	642	165	93
	5-10	5	2	4	4	7	2	281	0	71
	0-1	3	6	9	6	18	0	511	1	76
Ar2720	1-5	25	6	9	11	18	1	808	118	111
	5-10	42	7	7	4	20	1	991	231	170
	0-1	0	5	13	0	10	0	471	0	43
Yungay	1-5	0	1	5	0	3	0	520	0	59
	5-10	0	1	9	0	3	1	472	3	61

Table S3. The $\delta^{18}O_P$ values of HCl-extractable P for all sampling sites.

Site	Sampling depth		$\delta^{18}O_{HCl\text{-}P}$	SD	$\delta^{18}O_{HCl\text{-}P}$*	SD	$\delta^{18}O_{HCl\text{-}P}$ labeled water	SD
	cm		‰		‰		‰	
Ar1340	0-1	1	10.1	0.4				
		2	9.6					
	1-5	1	10.3	0.3				
		2	9.9					
	5-10	1	9.9	0.2				
		2	10.1					
Ar1680	0-1	1	10.8	0.8				
		2	12.2					
	1-5	1	14.2	0.5				
		2	13.6					
	5-10	1	12.4	0.1				
		2	12.3					
Ar2020	0-1	1	11.7	0.5				
		2	11.0					
	1-5	1	15.6	0.4	15.7	0.1	17.4	1.1
		2	16.1		15.8		15.8	
	5-10	1	24.0	0.2	24.1	0.9	25.5	0.9
		2	23.6		22.8		24.3	
Ar2455	0-1	1	10.1	0.1				
		2	10.3					
	1-5	1	10.5	0.1				
		2	10.6					
	5-10	1	11.9	0.0				
		2	11.9					
Ar2720	0-1	1	12.5	0.4				
		2	11.9					
	1-5	1	15.7	0.6				
		2	16.5					
	5-10	1	22.8	0.4				
		2	22.2					
Yungay	0-1	1	8.9	0.4				
		2	9.4					
	1-5	1	11.0	0.4				
		2	10.3					
	5-10	1	11.2	0.2				
		2	11.4					
Bedrock		1	10.6	0.9				
		2	9.4					

** Two of the samples with the highest content of HCl-P_o were extracted additionally with ^{18}O labeled 1M HCl solution to detect the potential incorporation of oxygen from the reagent via organic P hydrolysis. No significant $\delta^{18}O_{HCl\text{-}P}$ value differences were found between the same sample extracted by ^{18}O labeled and unlabeled HCl solutions.*

Fig. S1 The images for the soil profiles in the Aroma transect.

References:

Amphos 21 Consulting Chile L. (2013) *Analisis de Los Recursos Hidricos de La Quebrada de Aroma, Region de Tarapaca*., Ministrio de Obras Publicas. Available at: https://www.repositoriodirplan.cl:443/xmlui/handle/20.500.12140/25865.

Houston J. (2006) Variability of precipitation in the Atacama Desert: its causes and hydrological impact. *International Journal of Climatology* **26**, 2181–2198.

Moerchen R., Lehndorff E., Arenas Diaz F., Moradi G., Bol R., Fuentes B., Klumpp E., Amelung W. (2019) Carbon accrual in the Atacama Desert. *Global and Planetary Change* **181**, 102993